The surface characterization and bioactivity of NANOZR in vitro

著者	Han Jianmin
学位授与機関	Tohoku University
学位授与番号	11301乙第9238号
URL	http://hdl.handle.net/10097/57673

博士論文

The surface characterization and bioactivity of NANOZR *in vitro*

（ナノジルコニア表面性状と生体活性に関する基礎的研究）

平成 26 年度提出

東北大学大学院歯学研究科

口腔システム補綴学分野

（指導：佐々木 啓一 教授）

韓建民

ABSTRACT

1. PURPOSE:

The purpose of this study is to evaluate the biological behavior of MC3T3 cells on ceria-stabilized zirconia/alumina nanocomposite (NANOZR) in comparison to yttria-stabilized zirconia (3Y-TZP) and pure titanium.

2. METHODS

The NANOZR, 3Y-TZP and pure titanium disks 15mm in diameter and 1.5mm in thickness were used. The samples were polished with abrasive waterproof paper (400#, 600#, 800#). The three-dimension surface morphology and surface wettability were determined by scanning white light interferometry and surface contact angle meter, respectively. The cell proliferation was measured after seeding 1, 3, 7 and 14days by MTT method, cell morphology was measured at 1, 3 and 7 days by SEM， and the Alkaline phosphatase activity (ALP) was measured at 1, 3, 7, 14 and 21 days. Bovine serum albumin adsorption rate and cell skeleton were also examined at various times. All data were analyzed independently by one-way analysis of variance (ANOVA) combined with a Student-Newman-Keuls (SNK) multiple comparison test at a 5% level of significance.

3. RESULTS

The surface roughness of 3Y-TZP is higher than the NANOZR and pure titanium. The contact angle and cell proliferation has no significant difference among the three materials. The ALP expression of NANOZR is higher than the pure titanium and 3Y-TZP at 14 and 21 days although bovine serum albumin adsorption rate, cell morphology and cell proliferation was not different among the three materials.

4. CONCULSION

NANOZR has the comparable or preferable bioactivity as pure titanium. Within the limitation of this study, NANOZR has the reasonable potential as a substitution of the metal implant.

INTRODUCTION

Since Brånemark introduced the use of pure titanium for dental implantation 40 years ago [1)], titanium oral implants have been shown to function well for many years[2)]. In recent years, zirconia dental implants have been introduced into the market for the following reasons:

1) The dark color of a titanium implant can show through the pinkish hue of the cervical gingiva, especially in patients with a thin gingival biotype[3)]. The titanium can also become exposed if the soft tissue recedes. Zirconia is more compatible with esthetic requirements than titanium[4)].

2) Elevated titanium concentration in tissue have been reported in the vicinity of titanium oral implants[5)] and in regional lymph nodes[6)], which suggest that titanium may be a sensitinogen to some people[7)]. A review by Tschernitschek *et al.*[8)] concluded that products of titanium particle corrosion may provoke host reactions, and could be a potential health hazard. These findings prompt some patients to request treatment with completely metal-free dental reconstructions.

3) The zirconia has been used for manufacturing femoral heads for total hip replacements since the late 1980s[9)]. It has high mechanical strength and excellent tissue compatibility. Now it is being successfully used for crown and bridge restorations and dental ceramic abutments. Zirconia is also being evaluated as an alternative base material for endosseous oral implants.

Most of the zirconia used in dentistry is in the form of 3 mol% yttria-stabilized tetragonal zirconia polycrystals (3Y-TZP). In vitro and vivo studies have demonstrated that 3Y-TZP dental implants are comparable to titanium implants in terms of cell attachment, cell proliferation and histological response[10-15)]. The static fracture strength of a 3Y-TZP implant is between 725 N and 850 N, which is within the limits of clinical acceptability[16)]. However, 3Y-TZP may undergo low-temperature degradation (LTD) in the oral environment, and result in drastic failure of the implant[17)]. In addition, the fracture strength resistance of zirconia

implants may be reduced by the mode of preparation and cyclic loading[18]. These shortcomings need to be addressed before zirconia dental implants can be developed as a clinically successful alternative to titanium implants.

A Ce-TZP-based nanostructured zirconia/alumina composite (NANOZR) was developed by Nawa *et al.* in 1998[19,20]. The composite is composed of 10 mol% cerium dioxide (CeO_2) stabilized TZP as a matrix and 30 vol% of Al_2O_3 as a second phase. NANOZR exhibits greater flexural strength and fracture toughness than 3Y-TZP, and is completely resistant to low-temperature aging degradation[11,21]. Its cyclic fatigue strength is more than twice that of 3Y-TZP[22], indicating its suitability for use in dental implants.

Dental implant materials require good mechanical properties and the ability to rapidly and firmly integrate with the bone to function successfully in the long term. The osseointegration properties of biomaterials can be assessed by examining the behavior of osteoblasts on the implant surface. And examining the surface morphology and chemical-physical characteristics of material can assess the biological response of the tested materials. The aim of this study was to compare the performance of NANOZR, conventional 3Y-TZP, and pure titanium (CpTi) by assessing the surface 3D morphology, surface composition, wettability of these materials and bovine serum albumin adsorption rate, osteoblast-like cell attachment and morphology, proliferation kinetic, and ALP activity on the materials. This study on the behavior of osteoblast-like cell on implant materials *in vitro* provides an insight into their behavior during the osseointegration process *in vivo*.

MATERIALS AND METHODS

Specimen preparation

Disks 15 mm in diameter and 1.5 mm thick of NANOZR (Panasonic Health Care Co, Japan), 3Y-TZP (GC Co, Japan), and CpTi (Nippon Steel Co, Japan) were used in this study. The materials information in details is show in Table 1. A smooth surface was achieved by polishing with aluminum oxide waterproof abrasive paper (200#, 400#, 600#). The specimens were cleaned by sonication (SK3200LHC, KUDOS, China) in absolute acetone for 20 min, followed by immersion in ethanol for 10 min and ultrapure water for 3 min. Between preparation and analyses the specimens were stored in an airtight container.

Analyses of surface characterization

The surface topography of the specimens was examined with a microXAM-3D optical interferometer (KLA-Tencor Corp, Milpitas, CA) over an area of 0.6×0.8 mm^2 to measure the surface roughness (Ra). Three separate specimens were measured for each group, examining five representative sites on each specimen.

The specimens for SEM and EDX were gold-coated using Auto Fine Coaters (JFC-1600, JEOL Ltd., Tokyo, Japan) and observed with a Quanta 200 FEG scanning electron microscope (SEM; FEI, Eindhoven, Netherlands) associated with an energy dispersive x-ray analysis (EDX) to enable subtle comparison of the elemental composition. The surface morphology images were recorded at an accelerating voltage of 15 kV and 1000x magnification. Three separate specimens in each group were examined. Five random regions were imaged for each specimen.

The wettability of the specimens was determined using a portable contact angle meter (PCA-1; Kyowa Interface Science Co, Japan). An auto pipetter and a goniometer were employed to ensure uniformity of the distilled water droplet volume (2 μl). Images were analyzed with FAMAS software (Kyowa Interface Science Co,

Japan). All measurement was performed at room temperature with humidity of 50%. Two measurements were made on each of five separate specimens per substrate.

Analyses of bioactivities

In this study, MC3T3-E1 cells, osteoblast-like cell were used for evaluated the cell attachment, morphology, proliferation kinetic and ALP activity on the specimens. And the bovine serum albumin was used for evaluated the protein adsorption on the specimens.

The tested method of protein adsorption was referred to Hori[23]. The 300μl standard protein solution of bovine serum albumin (Wako Pure Chemical Industries Ltd., Japan) that prepared to 1 mg/ml (protein/ion-removed water) was pipetted onto surface of each sample. After incubated in sterile humidified condition at 37 °C for 1 hour, the surface was rinsed twice with water to remove the non-adherent protein. The removed and initial solution were mixed, 10 μl mixture was added to 200 μl Protein Assay Bradford Reagent (Wako Pure Chemical Industries Ltd., Japan) and waiting 5 min at room temperature. 150 μl reaction solution was transferred to 96 well plates. The amount of protein was quantified by a micro-plate reader (Bio-Rad Laboratories, Inc.) at 595 nm. The protein before and after adsorption was quantified by standard response curve produced by a consistent standard solution. The rate of protein adsorption was calculated as the percentage of protein adsorption on sample surface relative to the total amount of proteins initially applied.

For cell attachment and morphology, a 1.0 ml suspension with cell density of 1×10^4 cells/ml (MC3T3-E1: ATCC CRL-2594) was added to each well of a 24-well plate. The culture plate was transported gently to a 37 °C CO_2 incubator. After culturing for 4 hours, 1 day, 3 days and 7 days, the specimens were taken out, rinsed twice with phosphate-buffered saline solution (PBS, pH 7.2) to remove unattached cells, then fixed with 2.5% glutaraldehyde solution (G6257, Sigma, St. Louis, MO) for 30 min. The fixed cells were dehydrated progressively in a graded series of ethanols (50%, 75%, 90%, 99%) for 15 min. The specimens were sputter-coated with gold, and the cell morphology was observed by SEM.

For cell skeleton and nucleus observation, the attached cells were permeabilized with 0.2 % (v/v) Triton-X100 (Amresco, USA) for 4 min at room temperature followed by three rinses with PBS. Cells were then stained with rhodamine phalloidin (Cytoskeleton Inc., USA) at room temperature for 30 min, followed by three rinses with PBS, finally stained with DAPI-Fluoromount-G (Southern Biotech Co., USA). The cytoskeletal actin and cell nucleus were observed with laser scanning confocal microscopy (LSM 780, Zeiss Co., Germany). Three separate samples were examined for each group.

The quantity of attached cells was determined using the MTT (3-(4,5-dimethylthiazol-2-yi)-2,5-dipenyltetrazoliumbromic) method. A 1.0 ml suspension with cell density of 1×10^4 cells/ml was added to each well. After culturing for 1 day, 3 days, 7 days and 14 days, the specimens were rinsed twice with PBS (pH 7.2) to remove unattached cells, and 300 μl of MTT solution was added to each well. The plates were further incubated for 2 hours at 37 °C. The MTT solution was decanted and 300 μl of isopropanol was added to each well. After 30 min, 100 μl of the solution from each well was transferred to a 96-well plate and the optical density was measured using an enzyme labeling instrument (Model 680, BIO-RAD Laboratories Inc., Tokyo, Japan) at an excitation wavelength of 570 nm with 650 nm as the reference wavelength. Five separate specimens from each group were examined.

For the determination of ALP activity, a 1.0 ml suspension with cell density of 4×10^4 cells/ml was added to each well and pre-cultured for 3 days to achieve 100% cell conjugation. The cell culture medium was then replaced by differentiation medium (MK430, TaKaRa Biotechnology, Shiga, Japan), and further incubated. After culturing for 1 day, 3 days, 7 days, 14 days and 21 days, the specimens were rinsed twice with PBS (pH 7.2), and 200 μl ALP subscript buffer (pNPP, Sigma) and 2 μl 10%Triton X-100 were added to each well. The 24-well plate was placed in the CO_2 incubator for 15 min, followed by the addition of 150 μl/well of 2 mol/L NaOH to stop the reaction. Then 90 μl of the fluid from each well was transferred to a 96-well plate for optical density measurement using an enzyme labeling instrument

(Model 680, BIO-RAD Laboratories Inc., Tokyo, Japan) at 450 nm wavelength.

Statistic analysis

All data were analyzed independently by one-way analysis of variance (ANOVA) combined with a Student-Newman-Keuls (SNK) multiple comparison test at a 5% level of significance.

RESULTS

Surface characteristics of the specimens

Figure 1 shows the 3D topography of the three substrates surfaces as determined by a microXAM-3D optical interferometer. The titanium surface appears sharper than the zirconia surface. The surface roughness of the three substrates is around 0.3 μm (Figure 2), with no significant difference among them.

The SEM graphic of NANOZR, 3Y-TZP, and CpTi reveals similar surface scratching after polishing with 600# abrasive paper at 1000x magnification (Figure 3). The composition of the three materials is listed in Figure 4. CpTi is composed of titanium and oxygen, NANOZR is composed of zirconium, aluminum, oxygen, and cerium, while 3Y-TZP is composed of zirconium, oxygen, and ytterbium. All three materials also contain carbon.

Figure 5 shows that the surface contact angle against distilled water of the three substrates after cleaning with absolute acetone and ethanol is approximately 60°, with no significant difference among them.

Bioactivities of cells on the specimens

Figure 6 shows the three tested materials has similar albumin protein adsorption amount, there has no significant difference among them.

Figure 7 shows the general shape and growth pattern of MC3T3-E1 cells cultured on the three tested substrate materials. The seeding cells adhere properly to the tested materials. After 4 hours of incubation, the cells became flattened and did not spread completely on the surface, although the NANOZR and 3Y-TZP spread better than the CpTi. After 24 hours of incubation, the cells attached and spread well over the surface of all the materials. The cell morphology flattened to a spindle shape, and the cells on the surface of each substrate were connected with each. After 3 days of incubation, all the substrates showed greater density of osteoblasts with numerous cell-cell contacts, and with spindle cells along the scratches on the substrate

surface. After 7 days of incubation, the cells were 100% confluent, and completely covered the surface of the materials. There were no significant differences in the cell morphology of the three materials.

Figure 8 shows the actin cytoskeleton of MC3T3-E1 for various periods' incubation on three materials. There is similar fluorescence intensity of cells on three tested materials. After 1 hour incubation, the cell exhibited round, and had no obvious stress fibers and their actin fluorescence intensity was lower. After 4 hours incubation, the cells trend to spindle or polygonal morphology, and highly organized actin stress fibers were observed after 4 hours incubation, which indicating the strong cell adhesion. After 24 hours incubation, the cells on three tested materials show similar cytoskeleton.

Figure 9 shows the proliferation kinetic of MC3T3-E1 from 1 day to 14 days. We observed an exponential increase in cell numbers on all surfaces over the observation period. The number of cells attached to the three different surfaces within 1 day was almost identical, and the cell growth rate on the surface of the three materials was similar. The cells had a similar attachment and proliferation kinetic on the three substrate surfaces.

Figure 10 shows the ALP expression of the three substrates. ALP expression significantly increased 7 days after the differentiation culture, and increased during the 21-days test period. ALP expression was highest in NANOZR, followed by CpTi, while 3Y-TZP showed the lowest ALP expression. Before 7 days, there was no significant difference in ALP expression among the three substrates. At 14 days, the ALP expression of NANOZR and CpTi was significant higher than 3Y-TZP, while there was no significant difference between NANOZR and CpTi. At 21 days, there were significant differences among the three materials.

DISCUSSION

Zirconia has been used to manufacture femoral heads for total hip replacements since the late 1980s. Recently, zirconia has been broadly investigated *in vitro* and *in vivo* as dental implant. According to the authors, nearly almost of the studies showed that zirconia has high biocompatibility, all implants were osseointegrated without signs of inflammation or mobility. The biological response of zirconia showed at least equivalent or slightly better than pure titanium.

It is well known that surface composition, crystal size and surface morphology are major variables determining the cell response to the presence of an implant[24]. The surface morphology, especially the surface nano-morphology, can enhance cell bioactivity[25]. A granular surface can enhance the initial cell attachment, proliferation rate and expression of ALP[12,13]. The three materials examined in this study exhibit similar surface roughness and morphology, so the aim of this study become to compare the effect of the composition of the material substrates on the cellular response.

In vitro cell culture models for osteoblast behavior in response to implant materials, primary osteoblasts derived from rat calvaria or osteogenic osteosarcoma cell lines from animal and human bone are usually used, although occasionally primary human osteoblasts are also used. MG63 osteoblast-like cells derived from human osteosarcomas have frequently been used to evaluate the interaction of bone cells with implant biomaterials. However, it is not always possible to extrapolate the effects of osteosarcoma cell cultures to human bone cell cultures because they are tumor cell lines[26]. Moreover, Shapira *et al.*[27] compared the biological behavior of MG63 and Saos-2 cells on titanium surfaces, demonstrating that MG63 cells have non-differentiated properties (a high proliferative rate and low ALP activity), and are thus more closely related to pre-osteoblasts with an immature phenotype. A primary human cell culture system does not always exhibit reproducible results, owing to variations in phenotypic expression of cells from each isolate and the loss of the

osteoblastic phenotype with time in culture. Non-transformed cells from the MC3T3-E1 osteogenic cell line derived from newborn mouse calvaria[28] exhibited high ALP activity in the resting state and the capacity to differentiate into osteoblasts. Furthermore, these cells grew to form multiple cell layers[28]. Therefore, we selected the MC3T3-E1 cell line to examine NANOZR bioactivity response in this study.

General, the initial cell adhesion on the material surface occurs through mechanical interlocking, and the roughened surface improved early cell attachment. In the present study, the surface roughness of the three tested materials is between 0.3-0.4. In addition, there are some difference for the surface topography between NANOZR and pure titanium. However, the small difference for the surface roughness and surface topography may have no significant effect on the cell response to substrate materials, or the difference of cell response to the substrate materials can not detected by the present experimental technique.

From the results of XRD，we can see that all the three materials contain carbon element. We speculated that the carbon contamination is come from the accumulation of organic molecules, particularly those with a carbonyl moiety, which is considered unavoidable under ambient conditions. There has been reported that currently used implants, for clinical and experimental used, are found to contain hydrocarbons contaminated[29-32]. In the present study, although we try to remove the surface contamination by sonication in acetone and ethanol, there is still carbon element on the tested surface of materials used.

Surface wettability is one of the main factors reflecting the extent of cell adhesion onto the surface[33]. Many *in vitro* studies have investigated the relationship between the hydrophilicity of a material surface and cell adhesion. High surface wettability, which means a low contact angle, is generally reported to promote greater cell adhesion than a high contact angle[33-36]. The surface contact angles of the three tested substrates were not significantly different, which partly explains why the cell adhesion and proliferation dynamic of the three substrates were similar.

When material contact with medium containing serum, serum proteins can be immediately adsorbed onto the material surface prior to cell arrives. Therefore, the

adsorbed proteins play a mediator role in interactions between cells and tested materials[37,38]. The ability of the implant surface to adsorb proteins determines its aptitude to support cell adhesion and spreading[39]. The albumin is the most abundant in serum proteins, so we selected the albumin to examine the protein adsorption properties of materials in this study. The three tested materials show the similar protein adsorption ability. The protein adsorption is correlated to the surface composition, surface wettability, surface charge and surface topography[37]. In addition, the protein adsorption is also correlated to the surface roughness. The higher roughness, the bigger surface area, which means the higher protein adsorption value. From the results of this study, similar surface wettability, surface topography and surface roughness may partly explain similar albumin adsorption percentage among the three tested materials. However, in addition to the albumin, the bone derived cells attachment was mostly dependent upon the adsorption of vitronectin and fibronectin content[40,41]. Therefore, the adsorptions of vitronectin and fibronectin to material have needed to investigate in the further.

The visualization of cytoskeleton staining within 24 hours showed the initial contact of MC3T3-E1 with tested materials surface. There was no difference in cell morphology and adhesion among the NANOZR, 3Y-TZP and CpTi within 24h observation period. For all the tested materials, the osteoblast started to spread and developed focal adhesion contacts within 4 hours. The shape of most cells from round at initial contact within 1 hour to polygonal and spindle within 24 hours contact, while actin cytoskeleton trend to well organized. The fluorescent intensity and actin filaments expression is similar. This result is in concord with Yamashita *et al.*[12] reports, who demonstrated that the actin filaments distribution was similar on both zirconia and titanium. However, Hempel *et al.*[42] showed SAOS-2 cells on zirconia surface revealed a faster spreading and higher number of adherent cells compared with titanium after 24 hours incubation.

In this study, cell proliferation and cell morphology observed by SEM demonstrated appropriate adhesion and spreading of the cells on NANOZR, 3Y-TZP and CpTi. SEM observation revealed the close contact between the cell layers and the

three materials, confirming firm adhesion and anchorage of the cells. Such adhesive properties are important for cell proliferation and differentiation into bone forming cell. Cell proliferation and viability was determined using the MTT method，which relies on the mitochondrial activity of vital cells and represents a parameter for their metabolic activity. Cells seeded onto the three materials showed similar vitality and proliferation.

Both alumina and zirconia are chemically stable and bio-inert materials with similar bioactivity. In the present study, since NANOZR, 3Y-TZP and CpTi have similar cell adhesion and proliferation properties, the incorporated alumina and zirconia particles did not enhance the bioactivity response of MC3T3-E1 cells to the substrate. These findings are consistent with most of the published results. Bachle *et al.*[43] compared 3Y-TZP and CpTi using CAL72 osteoblast-like cells, and found that cell morphology and surface area covered by the cells were not affected by the type of substrate. Ko *et al.*[44] showed that zirconia/alumina has a higher proliferation rate than CpTi, and similar cell attachment and morphology. However, Depprich *et al.*[45] compared the acid etched zirconia surface to the titanium surface in relation to cell adhesion, proliferation, and the synthesis of bone-associated proteins. The cell adhesion and proliferation rate was significantly higher on the zirconia surface than on the titanium surface, but there was no difference in the synthesis of bone-specific proteins. Pandey *et al.*[46] reported that the stabilizer of zirconia maybe an influencing factor for its biocompatibility. The ceria stabilized zirconia probably reduce the biological activity compared to yttria stabilized zirconia. However, in this study, the ceria stabilized zirconia/alumina composite (NANOZR) showed similar biological activity with yttria stabilized zirconia (3Y-TZP). Carinci *et al.*[10] reported that alumina is able to affect the expression of some genes and proteinases. And Ko *et a.l*[44] reported that alumina has a higher proliferation rate than CpTi. Based on these reports, we suggest that the alumina, which NANOZR contained, might be the reason for this similar tendency in biological activity between NANOZR and 3Y-TZP.

In addition, NANOZR has a unique characteristic structure, that is several 10~100 nm sized Al_2O_3 particles are trapped within the ZrO_2 grains and several 10

nm sized ZrO_2 particles are trapped within the Al_2O_3 grains[21]. Webster *et al.*[47,48] and Wang *et al.*[13] reported that nano-sized grains can enhance protein interactions, osteoblast adhesion and proliferation. The biological activity of the microsurface can also be enhanced by nano-scale topography[13]. However, neither entrapped nano grain ZrO_2 nor Al_2O_3 had a significant effect on the surface energy and cell response. This may be attribute to the slight content of nanograins in NANOZR.

Bone ALP is a biochemical marker of the osteoblast phenotype in the stage of early differentiation, and hence also of bone formation and general osteoblast activity. This protein is also involved in the bone mineralization process[49]. In the present study, there was an obvious tendency towards an increased expression of ALP with the increasing culture time for the tested substrate. NANOZR recorded the highest ALP activity, possibly due to its chemical composition and topography. Boyan *et al.*[50] demonstrated that rough surface may enhance osteoblasts differentiation, and fine-tuning of the biomaterial surface topography may also possible control intracellular signaling events[51]. Oum'hamed *et al.*[52] and Carinci *et al.*[10] showed in their studies that zirconia, alumina, and titanium are able to upregulate or downregulate the expression of some genes and proteinases. We presume that the higher ALP expression of NANOZR maybe ascribes to its unique intergranular-type nanostructure, and ceria and alumina in NANOZR may also affect the osteoblast differentiation. This study tested only ALP activity, so further study is needed to clarify the effect of NANOZR on other bone-related proteins.

However, the results of cell culture studies are strongly dependent on the experimental conditions, and comparison between different studies is compromised. It is difficult to deduce the *in vivo* reaction of zirconia materials from present results. Further study is clearly needed to investigate the bioactivity of zirconia materials by different levels.

For a successful dental implant material, in addition to its superior biocompatibility and mechanical properties, the material should maintain stable and reliable performance under function environment. Despite the mechanical strength of NANOZR and 3Y-TZP maybe enough for mastication force, the wear and low

temperature aging of zirconia ceramic in vivo may induce the grain-pull out, increase surface flaw, and may decrease the properties of zirconia[21,53]. Some studies demonstrated that wear has a strong effect on aging of zirconia materials[54,55]. The hydrothermal aging may increase the roughness of zirconia, which in turn might increase the wear rate of counterpart. Moreover, the friction during function increases the aging rate of ziconia[55]. There is little information about wear of NANOZR, while NANOZR has superior resistance to low temperature aging than yttria stabilized zirconia (3Y-TZP) *in vitro*[21]. However, the intrinsic brittleness and high elastic modulus of zirconia ceramic may still restrict its wide use in implant dentistry. No-defect manufacturing process and bioactivity surface modifications is needed for future's zirconia implant.

CONCLUSIONS

1) Three test materials (NANOZR, 3Y-TZP and CpTi) basically had similar surface roughness, contact angle and cell viability.
2) ALP activities of MC3T3-E1 cells on NANOZR exceeded a little higher than CpTi and 3Y-TZP.
3) The three test materials (NANOZR, 3Y-TZP and CpTi) were biologically similar bio-inert materials.

ACKNOWLEDGEMENTS

My deepest gratitude goes first and foremost to Professor Keiichi SASAKI, my supervisor, for his constant encouragement and guidance. He led me into the world of NANOZR for dental implant. Without his consistent and illuminating instruction, this thesis could not have reached its present form.

Second, I would like to express my heartfelt gratitude to Professor Guang HONG, who has walked me through all the stages of the writing of this thesis. I am also greatly indebted to the Teachers at the department of Advanced Prosthetic Dentistry, such as Dr. Hiroyuki MATSUI and so on, who have instructed and helped me a lot in the past two years.

Last my thanks would go to my beloved family for their loving considerations and great confidence in me all through these years.

REFERENCE

1. Brånemark PI, Adell R, Breine U, Hansson BO, Lindström J, Ohlsson A. Intra-osseous anchorage of dental prostheses. I. Experimental studies. Scand J Plast Reconstr Surg 1969; 3: 81-100.
2. Adell R, Eriksson B, Lekholm U, Brånemark PI, Jemt T. Long-term follow-up study of osseointegrated implants in the treatment of totally edentulous jaws. Int J Oral Maxillofac Implants 1990; 5: 347-359.
3. Jung RE, Sailer I, Hammerle CH, Attin T, Schmidlin P. In vitro color changes of soft tissue caused by restorative materials. In J Periodontics Restorative Dent 2007; 27: 251-257.
4. Traini T, Pettinicchio M, Murmura G, Varvara G, Di Lullo N, Sinjari B, Caputi S. Esthetic outcome of an immediately placed maxillary anterior single-tooth implant restored with a custom-made zirconia-ceramic abutment and crown: a staged treatment. Quintessence Int 2011; 42: 103-108.
5. Bianco PD, Ducheyne P, Cuckler JM. Local accumulation of titanium released from a titanium implant in the absence of wear. J Biomed Mater Res 1996; 31: 227-234.
6. Weingart D, Steinemann S, Schilli W, Strub JR, Hellerich U, Assenmacher J, Simpson J. Titanium deposition in regional lymph nodes after insertion of titanium screw implants in maxillofacial region. Int J Oral Maxillofac Surg 1994; 23: 450-452.
7. Sicilia A, Cuesta S, Coma G, Arregui I, Guisasola C, Ruiz E, Maestro A. Titanium allergy in dental implant patients: a clinical study on 1500 consecutive patients. Clin Oral Implants Res 2008; 19: 823-835.
8. Tschernitschek H, Borchers L, Geurtsen W. Nonalloyed titanium as a bioinert metal--a review. Quintessence Int. 2005; 36: 523-530.
9. Christel P, Meunier A, Dorlot JM, Crolet JM, Witvoet J, Sedel L, Boutin P.

Biomechanical compatibility and design of ceramic implants for orthopedic surgery. Ann N Y Acad Sci 1988; 523: 234-256.

10. Carinci F, Pezzetti F, Volinia St, Francioso F, Arcelli D, Farina E, Piattelli A. Zirconium oxide: analysis of MG63 osteoblast-like cell response by means of a microarray technology. Biomaterials 2004; 25: 215-218.
11. Tanaka K, Tamura J, Kawanabe K, Nawa M, Oka M, Uchida M, Kokubo T, Nakamura T. Ce-TZP/Al_2O_3 nanocomposite as a bearing materials in total joint replacement. J Biomed Mater Res 2002; 63: 262-270.
12. Yamashita D, Machigashira M, Miyamoto M, Takeuchi H, Noguchi K, Izumi Y, Ban S. Effect of surface roughness on initial responses of osteoblast-like cells on two types of zirconia. Dent Mater J. 2009; 28: 461-470.
13. Ito H, Sasaki H, Saito K, Honma S, Yajima Y, Yoshinari M. Response of osteoblast-like cells to zirconia with different surface topography. Dent Mater J 2013; 32:122-129.
14. Gahlert M, Röhling S, Wieland M, Sprecher CM, Kniha H, Milz S. Osseointegration of zirconia and titanium dental implants: a histological and histomorphometrical study in the maxilla of pigs. Clin Oral Implants Res 2009; 20: 1247-1253.
15. Sennerby L, Dasmah A, Larsson B, Iverhed M. Bone tissue responses to surface-modified zirconia implants: A histomorphometric and removal torque study in the rabbit. Clin Implant Dent Relat Res 2005; 7: S13-20.
16. Andreiotelli M, Kohal RJ. Fracture strength of zirconia implants after artificial aging. Clin Implant Dent Relat Res 2009; 11: 158-166.
17. Chevalier J. What future for zirconia as a biomaterial? Biomaterials 2006; 27: 535-543.
18. Kohal RJ, Wolkewitz M, Tsakona A. The effects of cyclic loading and preparation on the fracture strength of zirconium-dioxide implants: an in vitro investigation. Clin Oral Impl Res 2011; 22: 808-814.
19. Nawa M, Nakamoto S, Sekino T, Niihara K. Tough and strong Ce-TZP/alumina nanocomposites doped with titania. Ceramic Int 1998; 24: 497-506.

20. Nawa M, Bamba N, Sekino T, Niihara K. The effect of TiO_2 addition on strengthening and toughening in intragranular type of 12Ce-TZP/Al_2O_3 nanocomposites. J Eur Ceram Soc1998; 18: 209-219.
21. Ban S. Reliability and properties of core materials for all-ceramic dental restorations. Japan Dent Sci Rev 2008; 44: 3-21.
22. Takano T, Tasaka A, Yoshinari M, Sakurai K. Fatigue strength of Ce-TZP/Al2O3 nanocomposite with different surfaces. J Dent Res 2012; 91: 800-804.
23. Hori N, Ueno T, Minamikawa H, Iwasa F, Yoshino F, Kimoto K, Lee MC, Ogawa T. Electrostatic control of protein adsorption on UV-photofunctionalized titanium. Acta Biomater 2010; 6: 4175-4180.
24. Anselme K. Osteoblast adhesion on biomaterials. Biomaterials 2000;21:667-81.
25. Wang G, Liu X, Zreiqat H, Ding C. Enhanced effects of nano-scale topography on the bioactivity and osteoblast behaviors of micron rough ZrO2 coatings. Colloids Surf B Biointerfaces 2011; 86: 267-274.
26. Clover J, Gowen M. Are MG-63 and HOS TE85 human osteosarcoma cell lines representative models of the osteoblastic phenotype? Bone 1994; 15: 585-591
27. Shapira L, Halabi A. Behavior of two osteoblast-like cell lines cultured on machined or rough titanium surfaces. Clin Oral Implants Res 2009; 20: 50-55.
28. Sudo H, Kodama HA, Amagai Y, Yamamoto S, Kasai S. In vitro differentiation and calcification in a new clonal osteogenic cell line derived from newborn mouse calvaria. J Cell Biol. 1983; 96:191-198.
29. Buser D, Broggini N, Wieland M, Schenk RK, Denzer AJ, Cochran DL, et al. Enhanced bone apposition to a chemically modified SLA titanium surface. J Dent Res 2004; 83: 529-533.
30. Massaro C, Rotolo P, De Riccardis F, Milella E, Napoli A, Wieland M, et al. Comparative investigation of the surface properties of commercial titanium dental implant. Part 1: chemical composition. J Mater Sci Mater Med 2002; 13: 535-548.
31. Takeuchi M, Sakamoto K, Martra G, Coluccia S, Anpo M. Mechanism of

photoinduced superhydrophilicity on the TiO2 photocatalyst surface. J Phys Chem B 2005; 109: 15422-15428.

32. Kikuchi L, Park JY, Victor C, Davies JE. Platelet interactions with calciumphosphate-coated surface. Biomaterials 2005; 2006: 5285-5295.
33. Park JY, Gemmell CH, Davies JE. Platelet interactions with titanium: modulation of platelet activity by surface topography. Biomaterials 2001; 22: 2671-2682.
34. Kubies D, Himmlová L, Riedel T, Chánová E, Balík K, Douděrová M, Bártová J, Pešáková V. The interaction of osteoblasts with bone-implant materials: 1. The effect of physicochemical surface properties of implant materials. Physiol Res 2011; 60: 95-111.
35. Noro A, Kaneko M, Murata I, Yoshinari M. Influence of surface topography and surface physicochemistry on wettability of zirconia (tetragonal zirconia polycrystal). J Biomed Mater Res B Appl Biomater 2013; 101: 355-363.
36. Kang G, Choee HJ, Rhee MH, Lee B. Interaction of different types of cells on physicochemically treated poly(L-lactide-co-glycolide) surface. J Appl Polym Sci 2002; 85: 1253-1262.
37. Wilson CJ, Clegg RE, Leavesley DI, Pearcy MJ. Mediation of biomaterial-cell interactions by adsorbed proteins: a review. Tissue Eng 2005; 11: 1-18.
38. Hlady V V, Buijs J. Protein adsorption on solid surfaces. Curr Opin Biotechnol 1996; 7: 72-77.
39. Kasemo B. Biological surface science. Surf Sci 2002; 500: 656-77.
40. Howlett CR, Evans MD, Walsh WR, Johnson G, Steele JG. Mechanism of initial attachment of cells derived from human bone to commonly used prosthetic materials during cell culture. Biomaterials 1994; 15: 213-222.
41. Curtis AS, Forrester JV. The competitive effects of serum proteins on cell adhesion. J Cell Sci 1984; 71: 17-35.
42. Hempel U, Hefti T, Kalbacova M, Wolf-Brandstetter C, Dieter P, Schlottig F. Response of osteoblast-like SAOS-2 cells to zirconia ceramics with different surface topographies. Clin Oral Implants Res 2010; 21: 174-181.

43. Bächle M, Butz F, Hübner U, Bakalinis E, Kohal RJ. Behavior of CAL72 osteoblast-like cells cultured on zirconia ceramics with different surface topographies. Clin Oral Implants Res 2007; 18: 53-59.
44. Ko HC, Han JS, Bächle M, Jang JH, Shin SW, Kim DJ. Initial osteoblast-like cell response to pure titanium and zirconia/alumina ceramics. Dent Mater 2007; 23: 1349-1355.
45. Depprich R, Ommerborn M, Zipprich H, Naujoks C, Handschel J, Wiesmann HP, Kübler NR, Meyer U. Behavior of osteoblastic cells cultured on titanium and structured zirconia surfaces. Head Face Med 2008; 8: 4-29.
46. Pandey AK, Pati F, Mandal D, Dhara S, Biswas K. In vitro evaluation of osteoconductivity and cellular response of zirconia and alumina based ceramics. Mater Sci Eng C Mater Biol Appl 2013; 33: 3923-3930.
47. Webster TJ, Siegel RW, Bizios R. Osteoblast adhesion on nanophase ceramics. Biomaterials 1999; 20: 1222-1227.
48. Webster TH, Ergun C, Doremus RH, Siegel RW, Bizios R. Enhanced functions of osteoblasts on nanophase ceramics. Biomaterials 2000; 21: 1803-1810.
49. Piattelli A, Scarano A,Corigliano M. Effect of alkaline phosphatase on bone healing around plasma-sprayed titanium implant: a pilot study in rabbits. Biomaterials 1996; 17: 1443-1449.
50. Boyan BD, Lossdörfer S, Wang L, Zhao G, Lohmann CH, Cochran DL, Schwartz Z. Osteoblasts generate an osteogenic microenvironment when grown on surfaces with rough microtopographies. Eur Cell Mater 2003; 6: 22-27.
51. Hamilton DW, Brunette DM. The effect of substratum topography on osteoblast adhesion mediated signal transduction and phosphorylation. Biomaterials 2007; 28: 1806-1819.
52. Oum'hamed Z, Garnotel R, Josset Y, Trenteseaux C, Laurent-Maquin D. Matrix metalloproteinases MMP-2, -9 and tissue inhibitors TIMP-1, -2 expression and secretion by primary human osteoblast cells in response to titanium, zirconia, and alumina ceramics. J Biomed Mater Res A. 2004; 68: 114-122.
53. Willmann G, Früh HJ, Pfaff HG. Wear characteristics of sliding pairs of

zirconia(Y-TZP) for hip endoprostheses. Biomaterials 1996; 17: 2157-2162.

54. Brown SS, Green DD, Pezzotti G, Donaldson TK, Clarke IC. Possible triggers for phase transformation in zirconia hip balls. J Biomed Mater Res B 2008; 85: 444-452.

55. Gremillard L, Martin L, Zych L, Crosnier E, Chevalier J, Charbouillot A, Sainsot P, Espinouse J, Aurelle JL. Combining ageing and wear to assess the durability of zirconia-based ceramic heads for total hip arthroplasty. Acta Biomater 2013; 9: 7545-7555.

Table 1. Material used in this study.

Code	Product name	Composition	Hardness (Vickers)	Flexural strength (MPa)	Fracture toughness (MPa $m^{1/2}$)	Manufacturer
NANOZR	P-NanoZR	70vol%10mol CeO_2-ZrO_2 30vol%Al_2O_3	1161	1500	18	Panasonic Electric Works
3Y-TZP	Aadva Zr	3mol Y_2O_3-ZrO_2	1250	1200	9.5	GC Corporation
CpTi	JIS H4600 TP270C Titanium Sheet	100% Ti	-	-	-	Nippon Steel Corporation

Note: The above details of tested materials were provided by manufacturers.

NANOZR

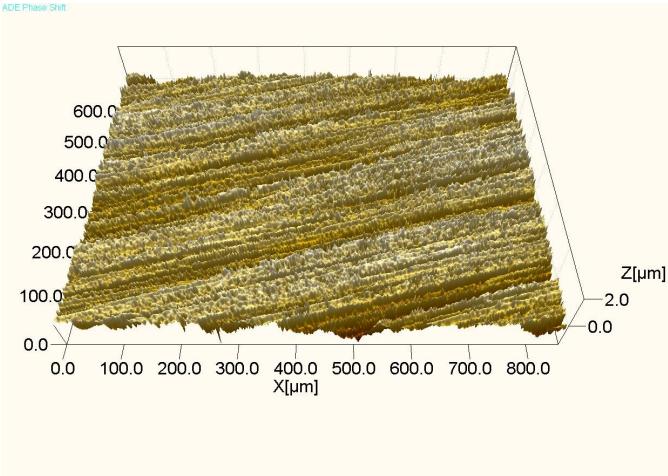

3Y-TZP

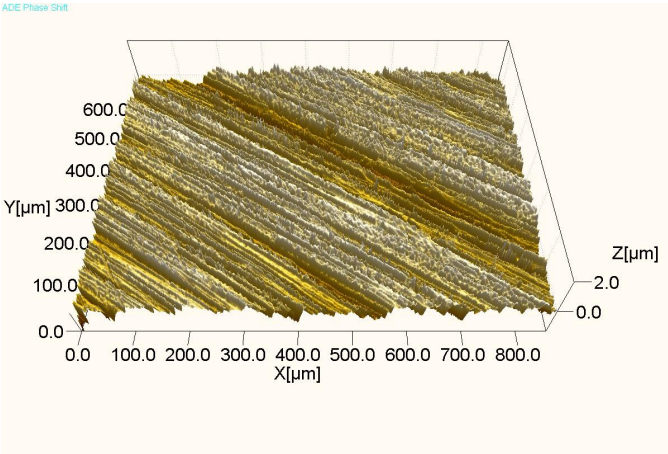

CpTi

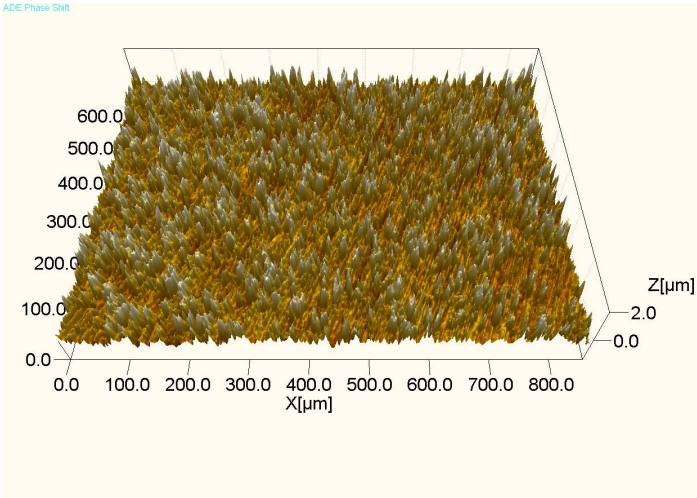

Fig. 1. 3D surface topography of NANOZR, 3Y-TZP and CpTi (0.6mm × 0.8mm) after polishing with 600# abrasive paper.

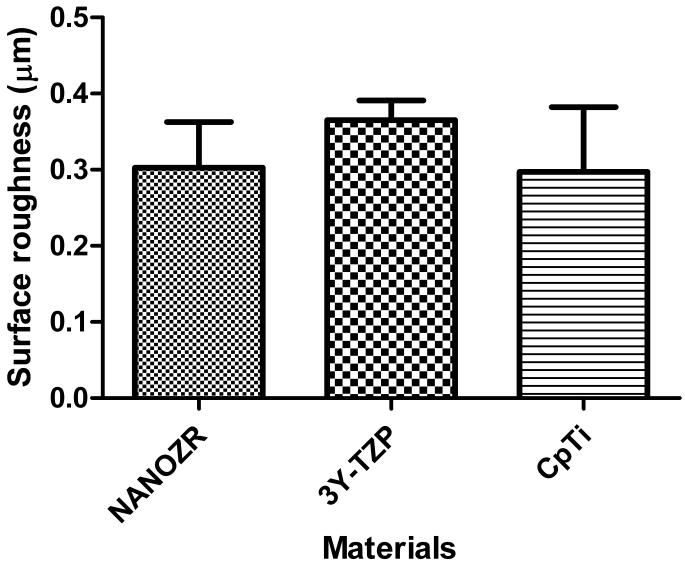

Fig. 2. Surface roughness of NANOZR, 3Y-TZP and CpTi after polishing with 600# abrasive paper.

There was no significant difference among the three materials (p>0.05).

NANOZR

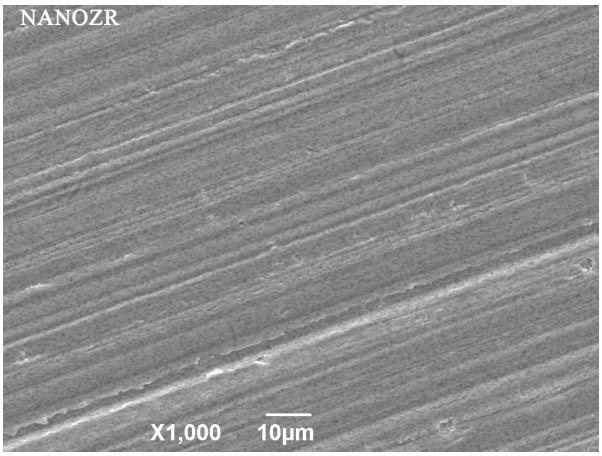

3Y-TZP

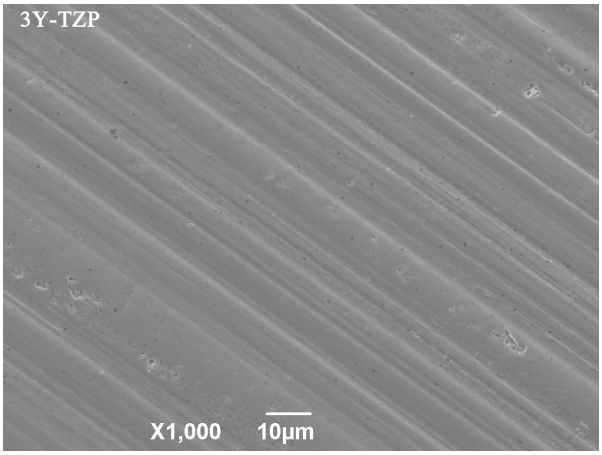

CpTi

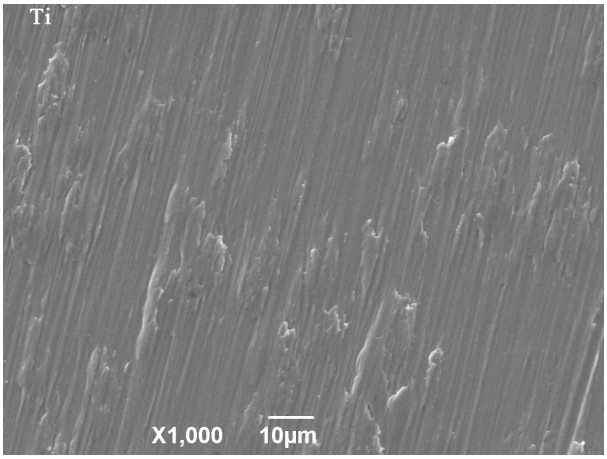

Fig. 3. SEM micrographs of NANOZR, 3Y-TZP and CpTi.

NANOZR

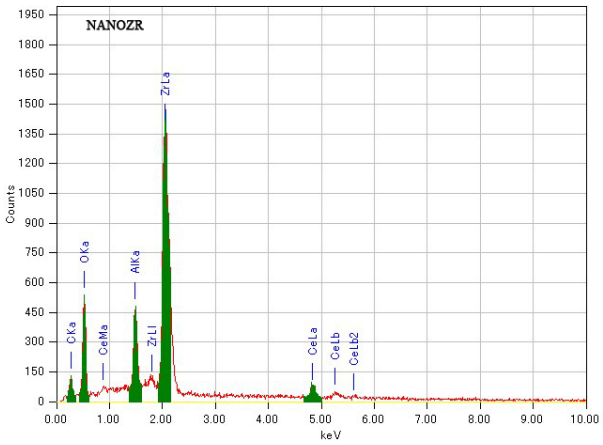

3Y-TZP

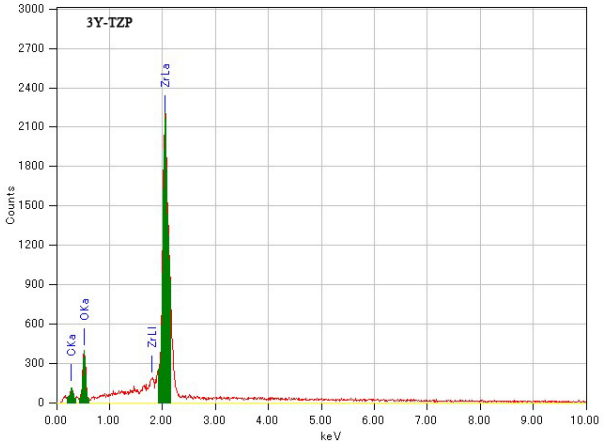

CpTi

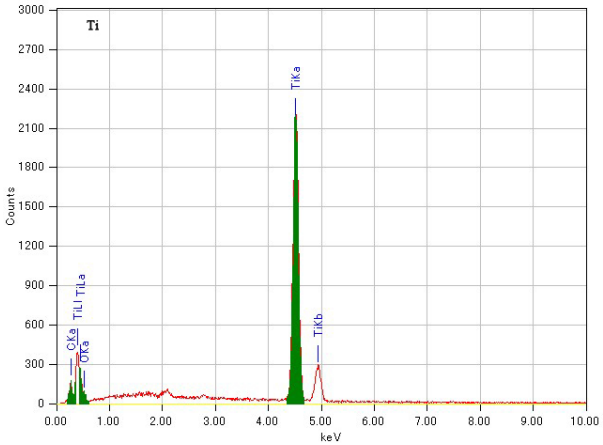

Fig. 4. Surface composition of NANOZR, 3Y-TZP and CpTi.

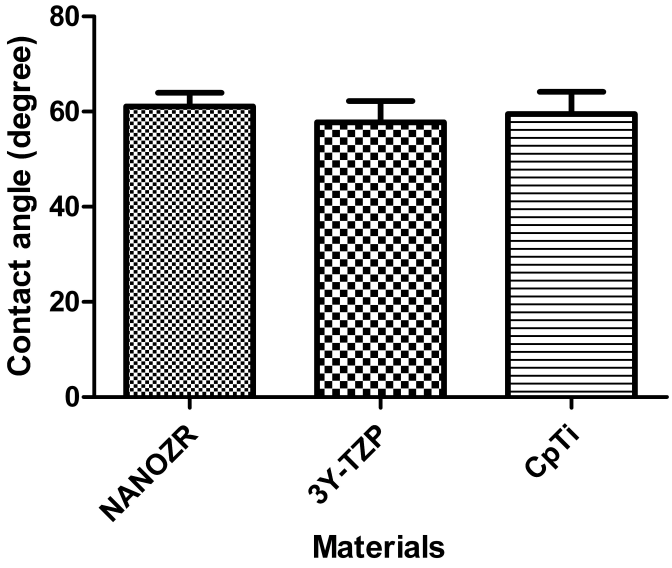

Fig. 5. Contact angle against distilled water of NANOZR, 3Y-TZP and CpTi.

There was no significant difference among the three materials (p>0.05).

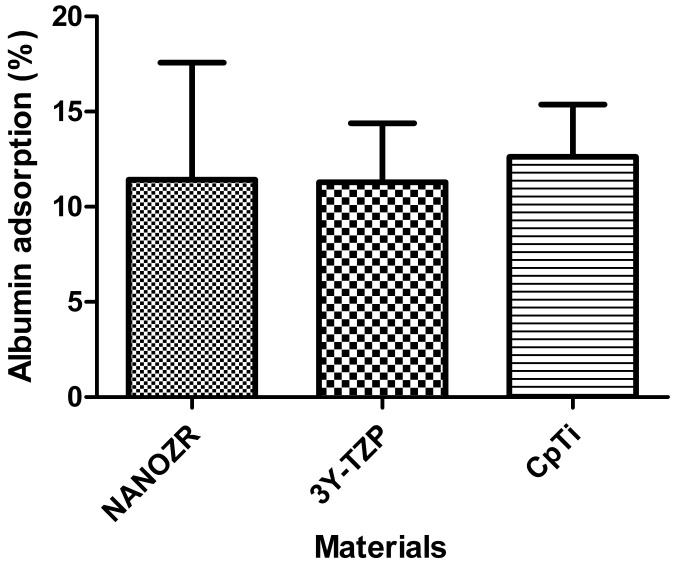

Fig. 6. Bovine serum albumin adsorption rates of NANOZR, 3Y-TZP and CpTi after 1 hour incubation. There was no significant difference among the three materials ($p>0.05$).

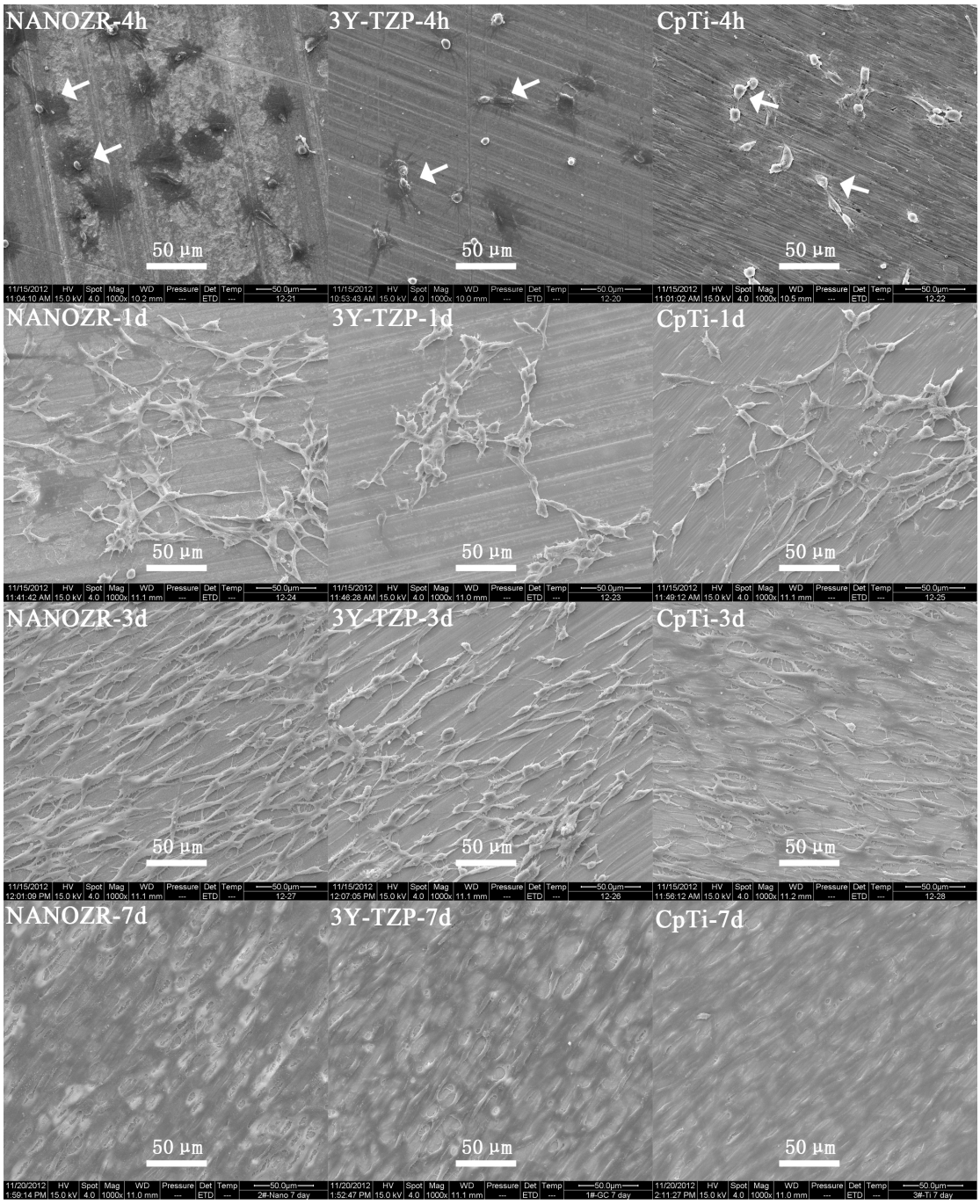

Fig. 7. SEM observation of MC3T3-E1 cells on NANOZR, 3Y-TZP and CpTi at 4hours, 1 day, 3 days and 7 days. Original magnification 1000×.

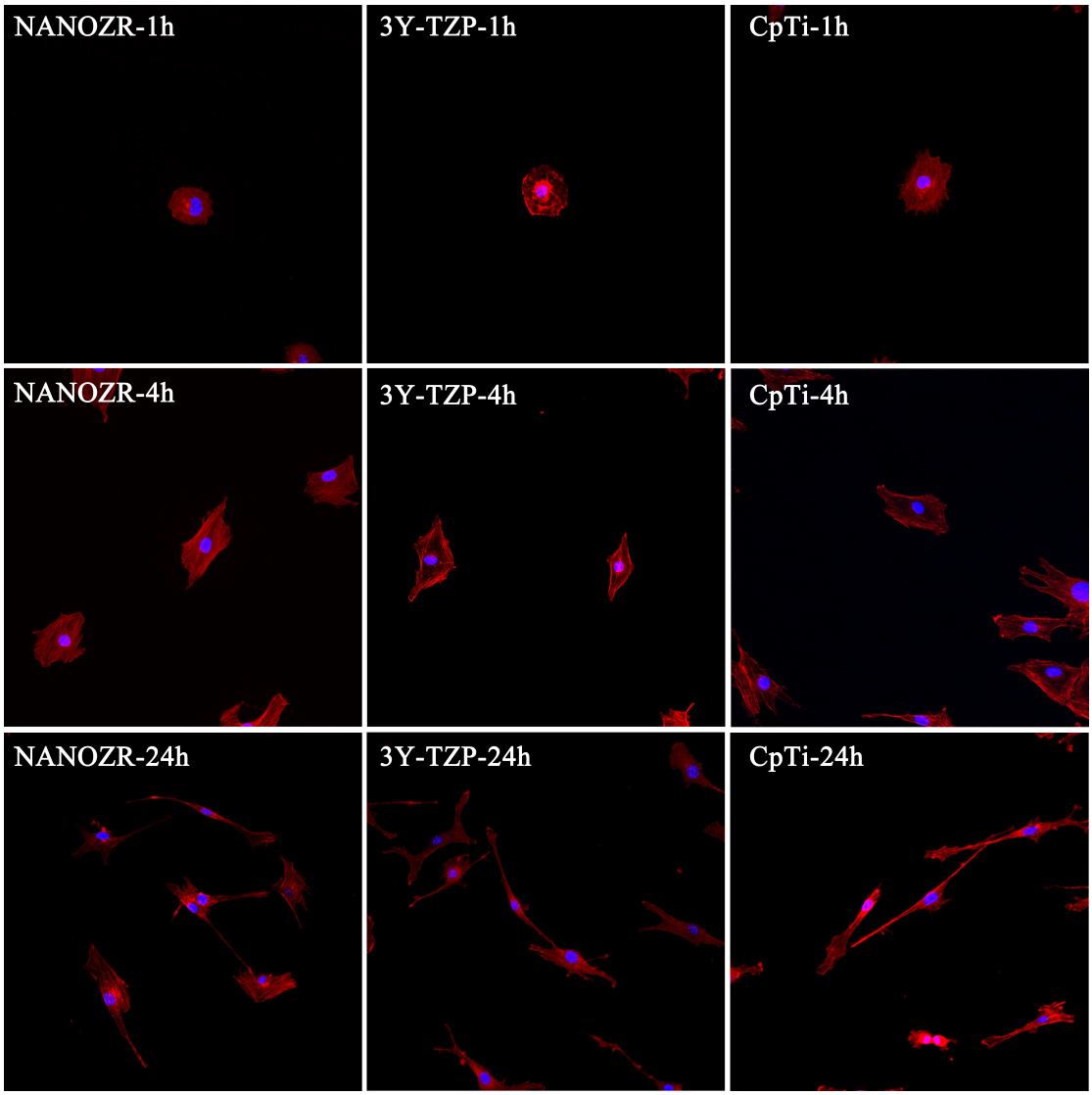

Fig. 8. Observation of actin cytoskeleton and cell nucleus of MC3T3-E1 on NANOZR, 3Y-TZP and CpTi after 1 hour, 4 hours and 24 hours incubation.

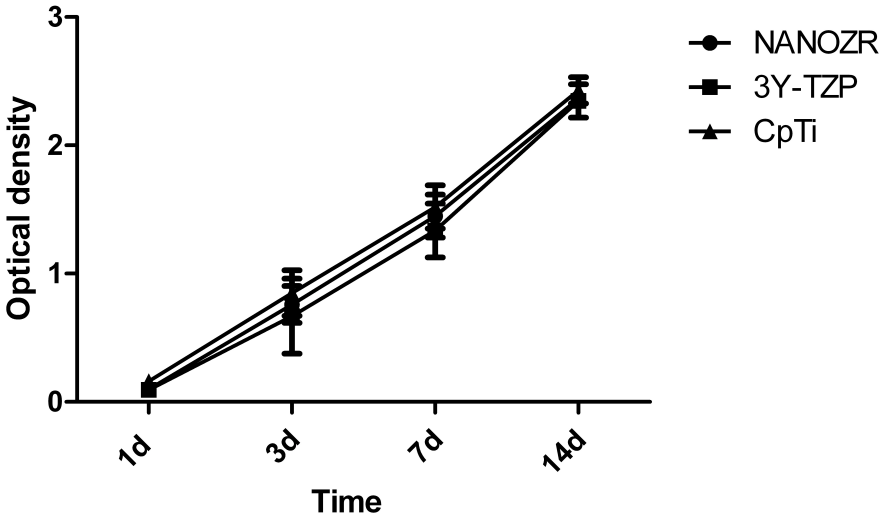

Fig.9. Cell proliferation kinetic of MC3T3-E1 cells on NANOZR, 3Y-TZP and CpTi at 1 day, 3 days, 7 days and 14days. There was no significant difference among the NANOZR, 3Y-TZP and CpTi within tested period (p>0.05).

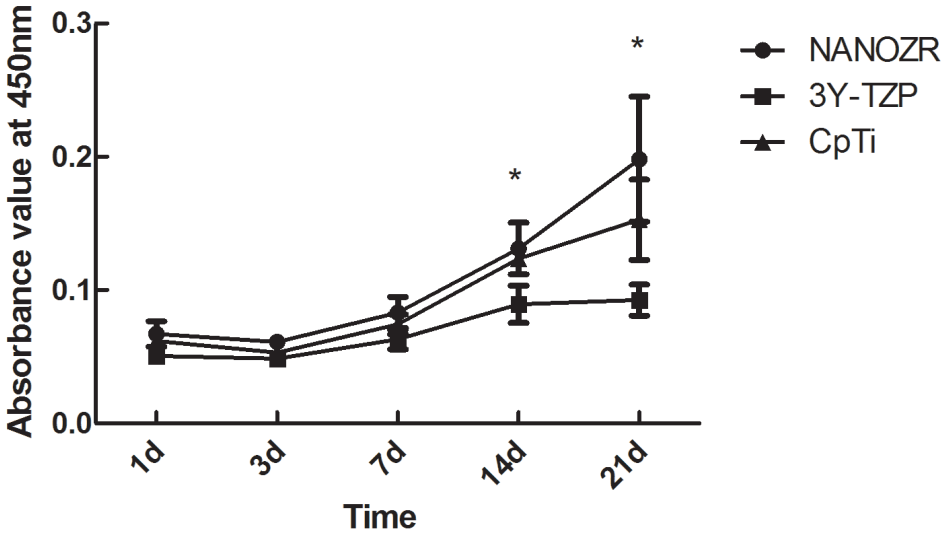

Fig.10. ALP expression of MC3T3-E1 cells on NANOZR, 3Y-TZP and CpTi at 1day, 3 days, 7 days, 14 days and 21days.

*: $p<0.05$, ANOVA.